

Growth model with restricted surface relaxation

T. J. da Silva and J. G. Moreira

*Departamento de Física, Instituto de Ciências Exatas,
Universidade Federal de Minas Gerais, Caixa Postal 702,
30161-970, Belo Horizonte, MG - Brazil*

(November 20, 2018)

We simulate a growth model with restricted surface relaxation process in $d = 1$ and $d = 2$, where d is the dimensionality of a flat substrate. In this model, each particle can relax on the surface to a local minimum, as the Edwards-Wilkinson linear model, but only within a distance s . If the local minimum is out from this distance, the particle evaporates through a refuse mechanism similar to the Kim-Kosterlitz nonlinear model. In $d = 1$, the growth exponent β , measured from the temporal behavior of roughness, indicates that in the coarse-grained limit, the linear term of the Kardar-Parisi-Zhang equation dominates in short times (low-roughness) and, in asymptotic times, the nonlinear term prevails. The crossover between linear and nonlinear behaviors occurs in a characteristic time t_c which only depends on the magnitude of the parameter s , related to the nonlinear term. In $d = 2$, we find indications of a similar crossover, that is, logarithmic temporal behavior of roughness in short times and power law behavior in asymptotic times.

I. INTRODUCTION

Self-affine interfaces generated by nonequilibrium surface growth have been intensively studied in recent years [1-3]. Kinetic roughening models as ballistic deposition⁴, Eden model⁵, solid-on-solid model (SOS) with surface relaxation^{6,7}, SOS with refuse⁸ and SOS with diffusion⁹ are some examples of growth models that belongs to distinct universality classes. Theoretically, these growth processes are studied in three different schemes: through a continuum description using Langevin-like equation and renormalization group analysis for solving it; through numerical solutions of these equations; and through computer simulations of discrete models. The main goal is to obtain the universality class of a specific model and to get information about the presence of nonlinearities and broken symmetries.

In computer simulation of lattice growth models, interfaces are described by a discrete set $\{h_i(t)\}$ which represents the height of a site i at the time t . Such an interface has L^d sites, where L is the linear size and d is the dimension of the substrate. The roughness of the interface ω is defined as the root mean square of the $\{h_i - \bar{h}\}$ distribution,

$$\omega^2(L, t) = \left\langle \frac{1}{L^d} \sum_{i=1}^{L^d} (h_i - \bar{h})^2 \right\rangle, \quad (1)$$

where \bar{h} is the mean height at time t and the angular brackets means the average over independent samples.

The universality class of a discrete growth model is obtained through the temporal and spatial behaviors of roughness. In the most of kinetic roughening processes, which starts at $t = 0$ from a flat substrate, the temporal behavior of roughness is described by the power law behavior, $\omega(L, t) \sim t^\beta$, when $1 \ll t \ll t_\times$, and its spatial behavior, in the steady state, is described by $\omega_{sat}(L) \sim L^\alpha$, for $t \gg t_\times$. The exponents β and α are the growth and roughness exponents, respectively, and t_\times is the saturation time. These two behaviors are joined at the Family and Vicsek dynamical scaling relation¹⁰

$$\omega(L, t) \sim L^\alpha f\left(\frac{t}{L^z}\right), \quad (2)$$

where the function $f(x)$ must be L -independent. This function scales as $f(x) \sim x^\beta$ for short times and tends to a constant in the steady state. The dynamical exponent z is related with α and β through the relationship $z = \alpha/\beta$ and it shows how the saturation time depends on the system size L : $t_\times \sim L^z$. Two of these exponents predict which universality class a model belongs to.

These universality classes are related to the dominant term of the stochastic differential equation in the continuum limit. In the next section, we describe two stochastic

differential equations which represent two distinct universality classes. The first is a linear equation proposed, in 1982, by Edwards and Wilkinson (EW equation)⁶. The second is a nonlinear equation, introduced by Kardar, Parisi and Zhang in 1986 (KPZ equation)¹¹. When the nonlinear term of this equation is null, the EW linear equation is recuperated.

In this article, we report on simulations of a growth model with restricted relaxation process (called RR model), which was proposed in order to study the crossover between the linear and nonlinear regimes of the KPZ equation. The RR combines features of the Edwards-Wilkinson (EW) model^{6,7}, related to the EW linear equation, and the Kim-Kosterlitz (KK) model⁸, related to the KPZ nonlinear equation. The crossover between linear and nonlinear regimes of the KPZ equation was studied numerically in $d = 1$ and $d = 2$ through numerical solutions of this equation where variations of the amount of nonlinearity was allowed. Moser and Kertész¹² found, in $d = 1$, the growth exponent $\beta = 1/3$ for all values of the nonlinearity. In $d = 2$, the authors have found $\beta = 0.240$, close to the Kim and Kosterlitz value⁸. So, a crossover between linear and nonlinear regimes was not verified. Grossmann, Guo and Grant¹³ also have obtained numerical solutions of KPZ equation where the surface tension was fixed and the nonlinear parameter was continuously changed. For small systems, the authors have found growth exponents in the interval $1/4 < \beta < 1/3$. So, the crossover was characterized by a continuum change in the growth exponent, which in $d = 1$ means that the dynamical exponent z depends on the amount of the nonlinearity. This continuous crossover in $d = 1$ was also verified by simulations on growth models^{14,15}. Theoretically, in $d = 1$, Nattermann and Tang¹⁶ have studied the KPZ equation in the low nonlinear limit through renormalization group analysis and they have obtained a different result: two behaviors separated by a characteristic time t_c . For $t \ll t_c$, the linear behavior of roughness was found, while for $t \gg t_c$, the nonlinearity dominates.

This article is organized in sections. The next section presents the general approach for kinetic roughening and describes the EW and KK models. In section III, we introduce the RR model and we show our results which confirm the theoretical previsions of Natterman and Tang¹⁶ and, in section IV, we finally show our conclusions.

II. THEORY AND DISCRETE MODELS

In the continuum (coarse-grained) description, the interface motion is described through Langevin-like equations [1-3],

$$\frac{\partial h(\mathbf{x}, t)}{\partial t} = v_0 + \eta(\mathbf{x}, t) + \Phi[h(\mathbf{x}, t)] \quad . \quad (3)$$

In this equation, v_0 and $\eta(\mathbf{x}, t)$ are the deposition rate and its noise, respectively. This white noise has zero mean and variance given by

$$\langle \eta(\mathbf{x}, t) \eta(\mathbf{x}', t') \rangle = D \delta^d(\mathbf{x} - \mathbf{x}') \delta(t - t'). \quad (4)$$

$\Phi[h(\mathbf{x}, t)]$ is the term related to the correlations between neighbors which can have linear and nonlinear functions of $h(\mathbf{x}, t)$.

Our interest is focused on the SOS model with surface relaxation^{6,7} and at the SOS model with restriction⁸. The SOS model with surface relaxation, introduced by Edwards and Wilkinson⁶ in 1982, is a random deposition of particles where the difference of height constraint between the neighbors $\{j\}$ of a site i is given by

$$h_i - h_{\{j\}} < M, \quad (5)$$

where M is the parameter that controls the roughness. In this work, we always use $M = 1$. If the height of the deposited particle on the site i does not satisfy the height constraint, this particle must be moved to a local minimum. Family⁷ have obtained for this model, in $d = 1$, the exponents $\beta = 0.25(1)$ and $\alpha = 0.48(2)$. This result indicates that this model, in a coarse-grained limit, belongs to the universality class defined by the EW equation

$$\frac{\partial h(\mathbf{x}, t)}{\partial t} = v_0 + \eta(\mathbf{x}, t) + \nu \nabla^2 h(\mathbf{x}, t), \quad (6)$$

where the laplacian term is related to the surface relaxation process. The exponents of this linear equation, obtained through Fourier analysis^{6,16}, are $\beta = 1/4$, $\alpha = 1/2$ and $z = 2$ for $d = 1$. For $d = 2$, which is the critical dimension of Eq.6, these exponents are $\beta = \alpha = 0$ which means that the roughness has logarithmic behavior in space and time ($\omega^2 \sim \log t$, for $t \ll L^z$, and $\omega_{sat}^2 \sim \log L$, for $t \gg L^z$). Both, the EW model and the EW equation, generate gaussian height distributions as well.

In the SOS model with restriction, particles are also randomly deposited onto a substrate and the difference of height constraint is the same of the EW model, Eq.5, but any kind of relaxation is allowed. If the height of a deposited particle does not satisfy Eq.5, this choice must be refused, that is, the particle evaporates. This model was proposed in 1989 by Kim and Kosterlitz⁸ in order to study nonlinear kinetic roughening in high dimensions. They numerically showed, in $d = 1$, that this model, named KK model, belongs to the universality class of the well known KPZ equation, proposed by Kardar, Parisi and Zhang¹¹

$$\frac{\partial h(\mathbf{x}, t)}{\partial t} = v_0 + \eta(\mathbf{x}, t) + \nu \nabla^2 h(\mathbf{x}, t) + \frac{\lambda}{2} [\nabla h(\mathbf{x}, t)]^2. \quad (7)$$

The appearance of the nonlinear term $[\nabla h(\mathbf{x}, t)]^2$ is due to the lateral growth, that is, the dependence of the

growth velocity on a local normal of the growing interface, or to the appearance of a perpendicular driven force that leads to a growth velocity greater or smaller than the deposition rate v_0 . In the case of the KK model, for example, the refuse mechanism makes the growth velocity smaller than the deposition rate. In $d = 1$, the exponents of this equation¹¹ are $\beta = 1/3$, $\alpha = 1/2$ and $z = 3/2$. In $d = 2$, the analytical solution is not known. In $d = 1$, numerical simulations of the KK model⁸ indicate $\beta = 0.332(5)$ and the α -exponent close to the expected value ($\alpha = 1/2$) and, in $d = 2$, $\beta = 0.250(5)$ and $\alpha = 0.40(1)$.

Eq.7 is not invariant under the $h \rightarrow -h$ transformation, which means that the up-down symmetry is broken in surfaces generated by a KPZ process. This fact leads to deviations in the gaussian character of the height distributions which can be measured using other moments of the distribution. The Eq.1 can be generalized for any moments of height distribution as

$$W_q(L, t) = \left\langle \frac{1}{L^d} \sum_{i=1}^{L^d} (h_i - \bar{h})^q \right\rangle, \quad (8)$$

where q is the order of the moment. Note that the roughness $\omega(L, t)$ is related to the second moment: $\omega^2(L, t) = W_2(L, t)$. A growing profile has up-down symmetry when positive and negative local curvatures are equals, and, in this case, $W_3(L, t)$ vanishes. On the other hand, when asymmetries are present, $W_3(L, t) \neq 0$. The skewness, defined by

$$S(L, t) = \frac{W_3(L, t)}{W_2^{3/2}(L, t)}, \quad (9)$$

is the ideal measurement of deviations from gaussian behavior. In the case of the EW model, $S(L, t) = 0$ always. For systems in KPZ class in $d = 1$, Krug *et al.*¹⁷ have indicated $|S(L, t)| \approx 0.28$ as an universal value in the transient state. In the steady state, the profile shows a random-walk character, that is, the height distribution is gaussian and $S_{sat}(L, t \gg t_x) = 0$. In $d = 2$, numerical simulations of the KK model indicate $S \approx -0.40$, in the transient state, and $S_{sat} \approx 0.28$, in the steady state^{18,19}.

III. MODEL DESCRIPTION AND RESULTS

In this article, we report on simulations of the growth model with restricted surface relaxation model (RR model). In the EW model, each incoming particle must search the local minima when the height constraint (Eq.5) is not satisfied. We introduce a parameter s that is the number of lattice units allowed for the relaxation process. If the deposited particle does not find the minimum after s relaxations, then this choice must be refused, as in KK model. For $s = 0$, the KK model is recuperated and $s \rightarrow \infty$ yields the EW model.

A. $d = 1$ Results

Figure 1 shows the log-log plot of roughness $\omega(L, t)$ vs time t for a system with $L = 10^5$ sites and $s = 2$. The time unity means L^d attempts of deposition. The two straight lines in the figure are showing the power-law fits with $\beta = 0.249(1)$ ($1 < t < 10^3$) and $\beta = 0.332(1)$ ($10^3 < t < 10^5$). The intersection of these two lines define the crossover time t_c . This crossover is easy to understand considering the increase of roughness: in short times, when the roughness is still small, particles do not need to relax very much for searching local minima, so the linear behavior might dominate. In large times, on the other hand, we note the appearance of relaxation lengths bigger than those observed in short times. As relaxation processes are linked to refuse processes in this model, the system undergoes a crossover to the nonlinear behavior. The crossover time t_c is independent of the system size L and it is only a function of the parameter s .

For a better understanding of this crossover we study the statistics of relaxations in the EW model, where relaxations of all sizes can occur. At the time t , be $\langle N_k(t) \rangle$ the mean number of particles which diffused k sites searching local minima. So, k relaxations occur with probability

$$P_k(t) = \frac{\langle N_k(t) \rangle}{L^d} . \quad (10)$$

These probabilities have an initial temporal dependence and a steady state $P_k(\infty)$, whose values are shown in Table 1. We note a strong decrease of the probability with the number of sites diffused, which shows the rare occurrences of the relaxation with large relaxation lengths.

It is interesting to analyse the approach of this probability to the steady state because each $P_k(t)$ has different convergence times. For doing this, we define a normalised probability of k relaxations as

$$p_k(t) = \frac{P_k(t)}{P_k(\infty)} . \quad (11)$$

Figure 2 shows the plots of $p_k(t)$ vs t for $k = 0; 1; 2; 3; 4$ for the EW model with $L = 10^5$. Note the differences among the convergences to each steady state: the temporal behaviors of p_0 and p_1 quickly go to its steady values, while p_2 and p_3 tend to unity only at $t \approx 10^3$ and $t \approx 10^4$, respectively. This fact suggests that large relaxation lengths might occur at large deposition times with small probabilities. So, drawing attention to the curve $p_2(t)$ vs t , we observe that the saturation occurs at $t \approx 10^3$. In the RR model with $s = 2$, we estimate $t_c \approx 10^3$, which indicates that the crossover from linear to nonlinear behaviors of the RR model occurs, for a value of s , when $p_{k=s}(t)$ is time independent.

This behavior of p_k is responsible for the dependence of the crossover time t_c with the parameter s in the RR model. Figure 3 shows clearly this dependence with the

plots of $\omega(L, t)/t^\beta$ vs t for: (a) $\beta = 1/4$ and (b) $\beta = 1/3$, with $s = 0, 2, 4$ and $L = 10^5$. In (a), the curve with $s = 0$ always grows, while the curve for $s = 4$ remains constant, indicating that $\beta = 1/4$, for this value of L , is the correct value for $s = 4$ (EW behavior) and a noncorrect for $s = 0$ (KK nonlinear behavior). In (b) similar conclusions are obtained with $\beta = 1/3$. For $s = 2$, the initial linear and the asymptotic KPZ behaviors are well observed in (a) and (b), respectively. Note that the crossover for $s = 2$ occurs when the $p_2(t)$ is time independent, that is, when $p_2(t) \approx 1$, in Figure 2. For $s = 4$, we observe only the linear behavior because the total deposition time is smaller than the crossover time t_c .

In order to do a more complete characterization of this crossover, we also analyse the temporal behavior of the skewness $S(L, t)$. Figure 4 shows plots of $S(L, t)$ vs t for $L = 10^5$ and several values of the parameter s . For $s = 0$, the skewness $S(t)$ goes quickly to the KPZ transient value $S = -0.28$. As we have explained, $S \neq 0$ means that the interfaces have not up-down symmetry. We find for $s = 2$, a slower approach to the KPZ value, than observed for $s = 0$, indicating that the up-down symmetry is gradually lost when $s > 0$. In particular, for $s = 3$, we clearly observe an initial behavior where $S \approx 0$ and an approach faster to the KPZ value at $t \approx 10^4$. The temporal dependence of $S(L, t)$, which is an independent measurement of the universality class, also indicates an initial linear behavior and the KPZ behavior in asymptotic times.

B. $d = 2$ Results

It is also interesting to study this crossover in $d = 2$, because changes in the morphology are expected in this dimension. For the KK model, we have power-law divergencies of roughness ($\omega^2 \sim t^{0.50}$ and $\omega^2 \sim L^{0.78}$), while the EW model shows logarithmic divergencies ($\omega^2 \sim \ln t$ and $\omega^2 \sim \ln L$).

In order to avoid saturation effects, we work with $L = 2000$ (4×10^6 sites), and we do simulations until $t = 10^4$. Due to the computational cost, we perform only two samples for each value of the parameter s and, consequently, the data quality in this section is poorer than in the previous subsection. The crossover is analysed through a similar process done in $d = 1$. We expect logarithmic behavior when the linear term dominates, so we define

$$Y_s(t) = \frac{\omega^2(t) - B_s}{A_s \ln(t)} , \quad (12)$$

where A_s and B_s are the s -dependent coefficients obtained through a logarithmic regression in the interval $2 < t < 100$. In Figure 5, we plot the temporal behavior of the function $Y_s(t)$, in a semi-logarithmic scale. If the temporal behavior of the roughness is logarithmic, $Y_s(t)$ must be a constant, equal to one. We note that

this occurs for $s = \infty$, but, for $s = 1$, this constant behavior remains until $t \approx 10^2$. After this time, there is a crossover to the power law behavior. However, until the studied time, it is not possible to determine the exponent.

In order to verify the existence of a power law behavior with the KPZ exponent β , we need to analyse values of the parameter s smaller than $s = 1$, that is, we need to do continuum variations in s . So, we do this by assing a probability s for the particle relax one lattice unit and a probability $(1 - s)$ for the particle be evaporated. In figure 6, we show the graph of ω/t^β vs t , for $s = 0$ (KK model) and $s = 0.1, 0.3, 0.5$. In this graph, it was used $\beta = 1/4$ which is the exponent for the KK model in $d = 2$ ⁸. If the temporal behavior of the roughness has a power law behavior with this exponent, the curves must be horizontal. For the RR model ($s \neq 0$), the curves show asymptotic approaches to this nonlinear behavior. For greater values of the parameter s , the crossover time to this behavior occurs for times greater than the time studied ($t = 10^4$).

IV. CONCLUSIONS

We have studied the model with restricted surface relaxation which combines the main features of the model with surface relaxation (EW model) and the model with refuse (KK model). A power-law temporal behavior of roughness with two growth exponents was observed in $d = 1$: The linear growth exponent, $\beta = 1/4$, occurs in short times and the nonlinear one, $\beta = 1/3$, appears in the asymptotic limit. This result suggests the following description: the linear term of the KPZ equation (Eq.7) dominates in short times and the nonlinear term dominates in asymptotic times. We also noted that the crossover time t_c is independent of the system size L and it is only function of the parameter s . This result corroborates the renormalization group solution made by Nattermann and Tang¹⁶, where the KPZ equation with small nonlinear term was considered. In $d = 2$, we have found indications of the same kind of crossover: A logarithmic temporal behavior of roughness in short times, which is related to the linear EW equation, and a power-law behavior with $\beta = 0.25$ in asymptotic times, related to the nonlinear KPZ equation.

Acknowledgments

The authors would like to thank Rogério Magalhães Paniago for a critical reading of the manuscript. The simulations were made at an ensemble of Digital Alpha 500 Au of the Departamento de Física -UFMG and at a Sun HPC 10000 of the CENAPAD MG-CO. This work was supported by CNPq, Fapemig and Finep/Pronex, Brazilian agencies.

- ¹ P. Meakin, *Fractals, Scaling and Growth Far from Equilibrium*, Cambridge Univ. Press, Cambridge (1998).
- ² A.-L. Barabási and H. E. Stanley, *Fractal Concepts in Surface Growth*, Cambridge Univ. Press, Cambridge (1995)
- ³ J. Krug, *Adv. Phys.* **46**, 139 (1997).
- ⁴ M. J. Vold, *J. Phys. Chem.* **64**, 1616 (1960). P. Meakin, P. Ramanlal, L. M. Sander and R. C. Ball, *Phys. Rev. A* **34**, 5091 (1986).
- ⁵ M. Eden, *Proc. Fourth Berkeley Symp. Mathematical Statistics and Probability, Volume IV*. Edited by L. Le Cam and J. Neyman: *Biology and Problems of Health* (University of California Press, Berkeley, 1961).
- ⁶ S. F. Edwards and D. R. Wilkinson, *Proc. R. Soc. A* **381**, 17 (1982).
- ⁷ F. Family, *J. Phys A* **19**, L441 (1986).
- ⁸ J. M. Kim and J. M. Kosterlitz, *Phys. Rev. Lett.* **62**, 2289 (1989).
- ⁹ D. E. Wolf and J. Villain, *Europhys. Lett* **13**, 389 (1990).
- ¹⁰ F. Family and T. Vicsek, *J. Phys. A* **18**, L75 (1985).
- ¹¹ M. Kardar, G. Parisi and Y.-C. Zhang, *Phys. Rev. Lett.* **56**, 889 (1986).
- ¹² K. Moser, J. Kertész and D. E. Wolf, *Physica A* **178**, 215 (1991).
- ¹³ B. Grossmann, H. Guo and M. Grant, *Phys. Rev. A* **43**, 1727 (1991).
- ¹⁴ H. Yan, D. Kessler and L. M. Sander, *Phys. Rev. Lett.* **64**, 926 (1990).
- ¹⁵ Y. P. Pellegrini and R. Jullien, *Phys. Rev. Lett* **64**, 1745 (1990); *Phys. Rev. A* **43** 920 (1991).
- ¹⁶ T. Nattermann and L.-H. Tang, *Phys. Rev. A* **45**, 7156 (1992).
- ¹⁷ J. Krug, P. Meakin and T. Halpin-Healy, *Phys. Rev. A* **45**, 638 (1992).
- ¹⁸ Y. Shim and D. P. Landau, *Phys. Rev. E* **64** No 036110 (2001).
- ¹⁹ C.-S. Chin and M. den Nijs, *Phys. Rev. E* **59**, 2633 (1999); M. Prähofer and H. Spohn, *Phys. Rev. Lett.* **84**, 4882 (2000);
- ²⁰ J. Krug and P. Meakin, *J. Phys. A* **23**, L987 (1990).
- ²¹ S. Pal and D. P. Landau, *Physica A* **267**, 406 (1999).

Figure captions

Figure 1

The temporal behavior of the roughness $\omega(L, t)$ for the RR model simulated at a substrate with $L = 10^5$ sites and $s = 2$, in a log-log plot. The two straight lines are showing the power-law fit results with $\beta = 1/4$ (short times) and $\beta = 1/3$ (asymptotic times). The crossover time t_c is defined as the intersection of these two lines, as indicated in the figure.

Figure 2

The temporal behavior of normalised probability of k relaxations $p_k(t)$ for the EW model with $L = 10^5$ sites for $k = 0; 1; 2; 3; 4$, from top to below.

Figure 3

The log-log plots of temporal behaviors of: (a) $\omega/t^{1/4}$ and (b) $\omega/t^{1/3}$ for $s = 0; 2; 4$ and $L = 10^5$. We might observe, for $s = 2$, when the system drives away from the linear behavior in (a) and, the arrival at the nonlinear KPZ behavior in (b). For $s = 4$, the system must approach to the KPZ behavior at deposition time greater than $t = 10^5$.

Figure 4

The temporal behavior of the skewness $S(L, t)$ for $L = 10^5$ for several values of the parameter s . The two horizontal lines show the value $S = 0$ (EW value) and $S = -0.28$ (KPZ value).

Figure 5

The temporal behavior, in a semi-logarithmic scale, of the function $Y_s(t)$ for $s = 1$ and $s = \infty$ (EW) with $L = 2000$. The dashed horizontal line indicates the constant value $Y_s(t) = 1$.

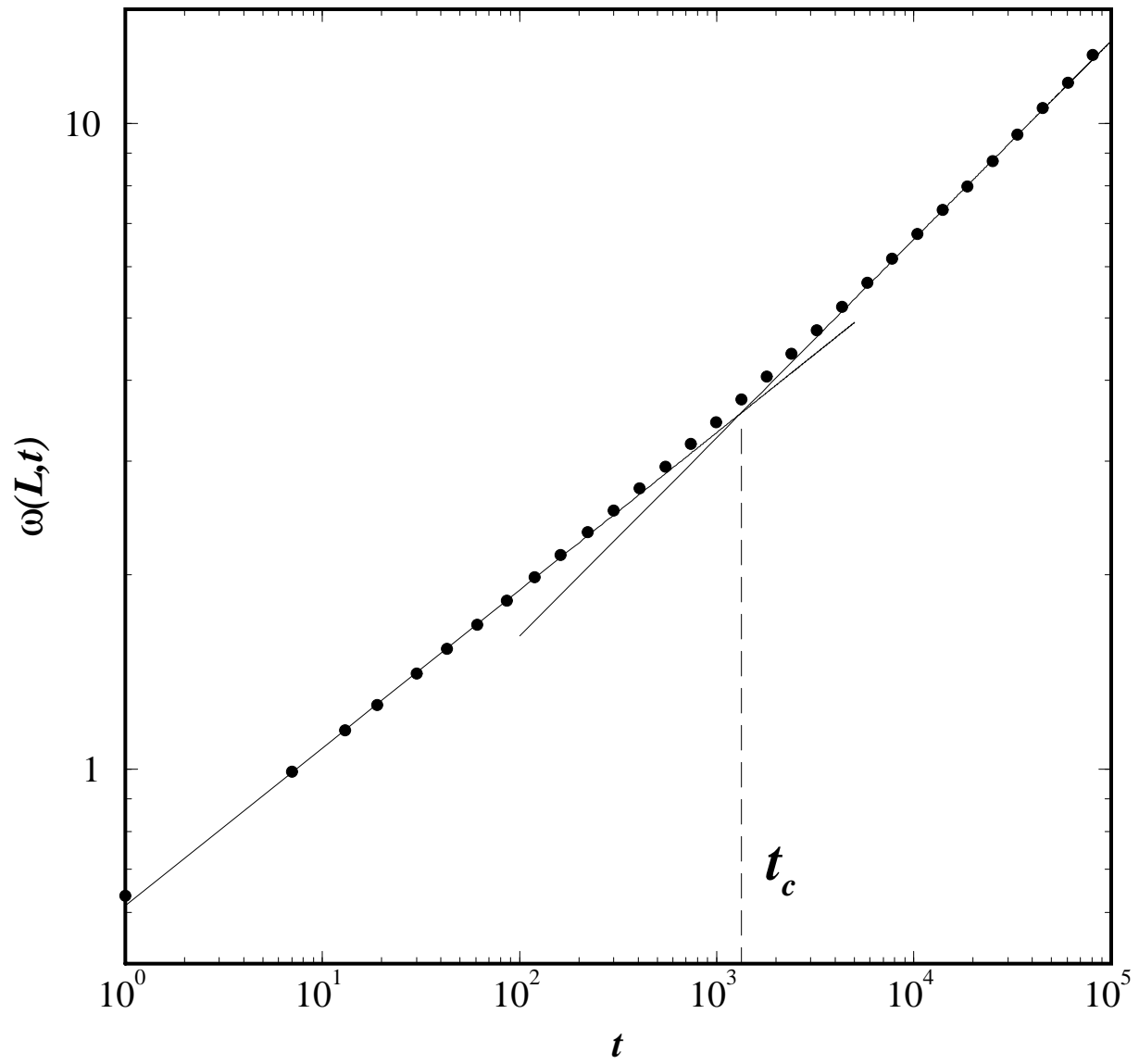
Figure 6

The semi-logarithmic graph of $\omega(L, t)/t^{1/4}$ in function of the time t for $L = 2000$ and some values of the parameter s .

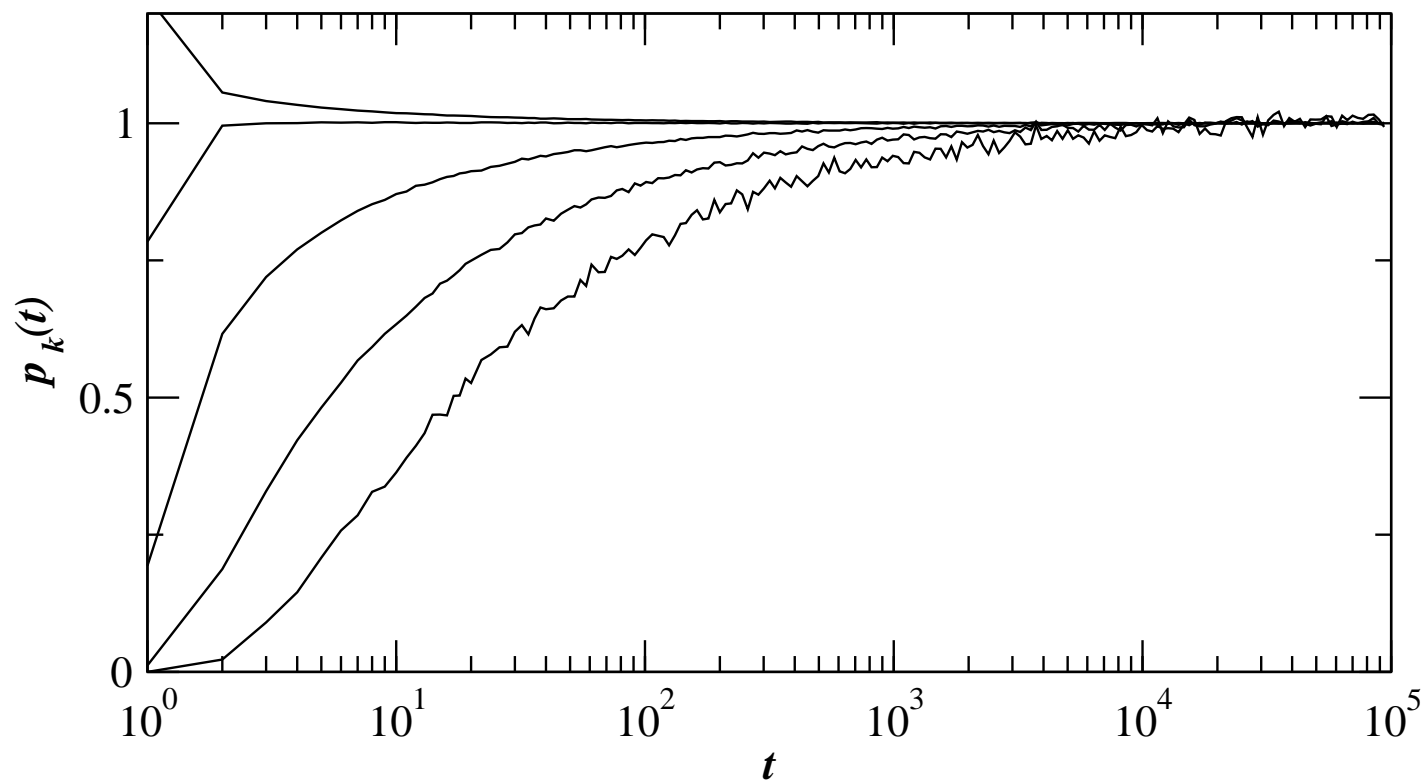
TABLE 1

k	$P_k(\infty)$
0	0.5813(3)
1	0.3481(3)
2	0.0616(1)
3	0.00812(2)
4	0.00085(1)
5	$7(5) \times 10^{-5}$

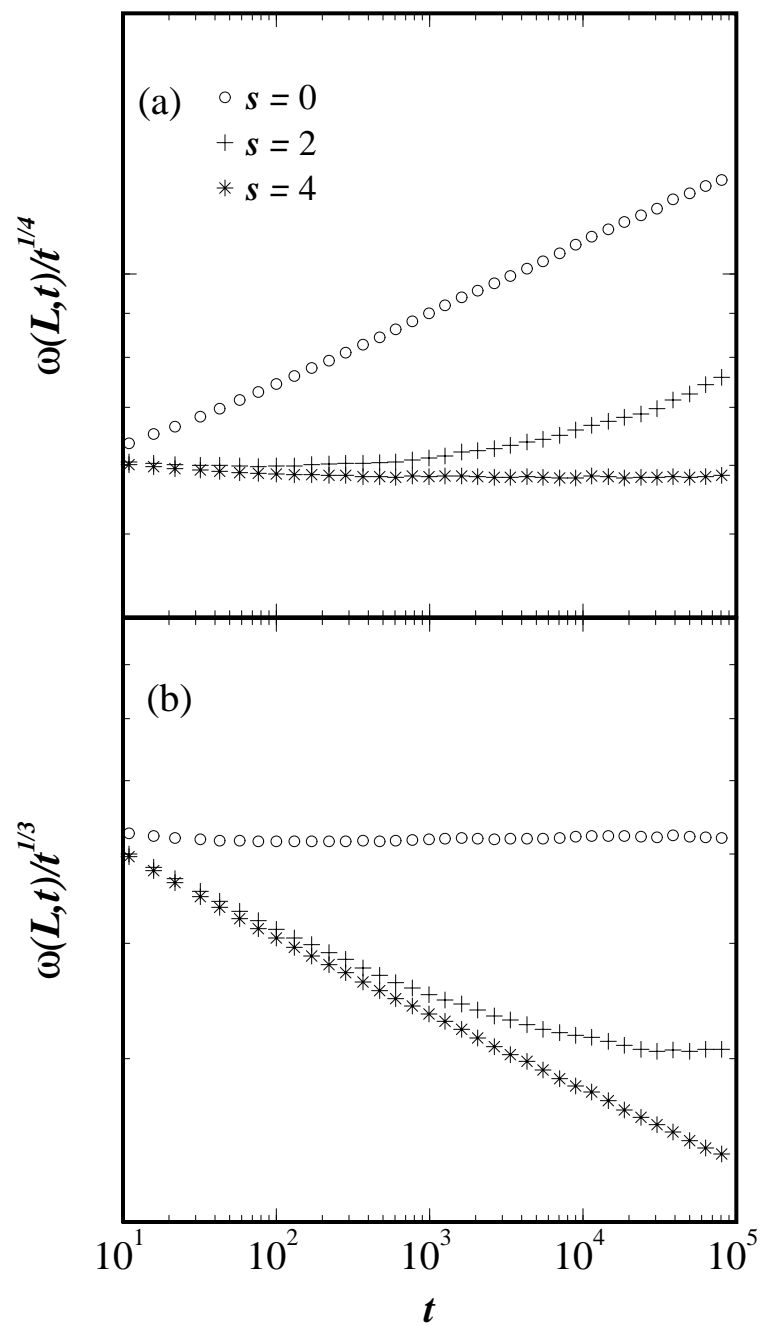
The steady state values of probability of diffusion k sites determined as the mean value in the interval $10^4 \leq t \leq 10^5$ for a EW system with $L = 10^5$.



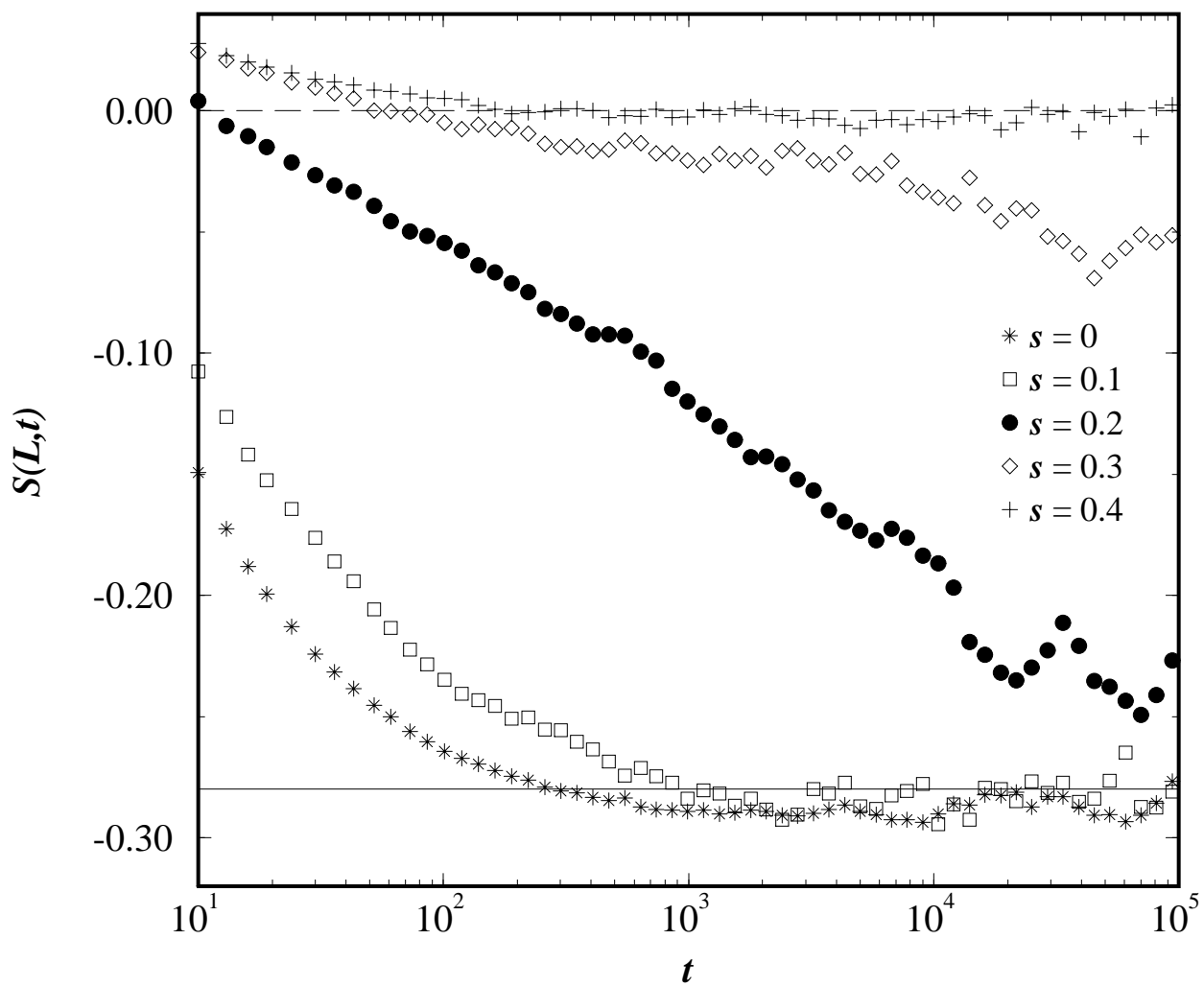
T. J. da Silva and J. G. Moreira - Figure 1



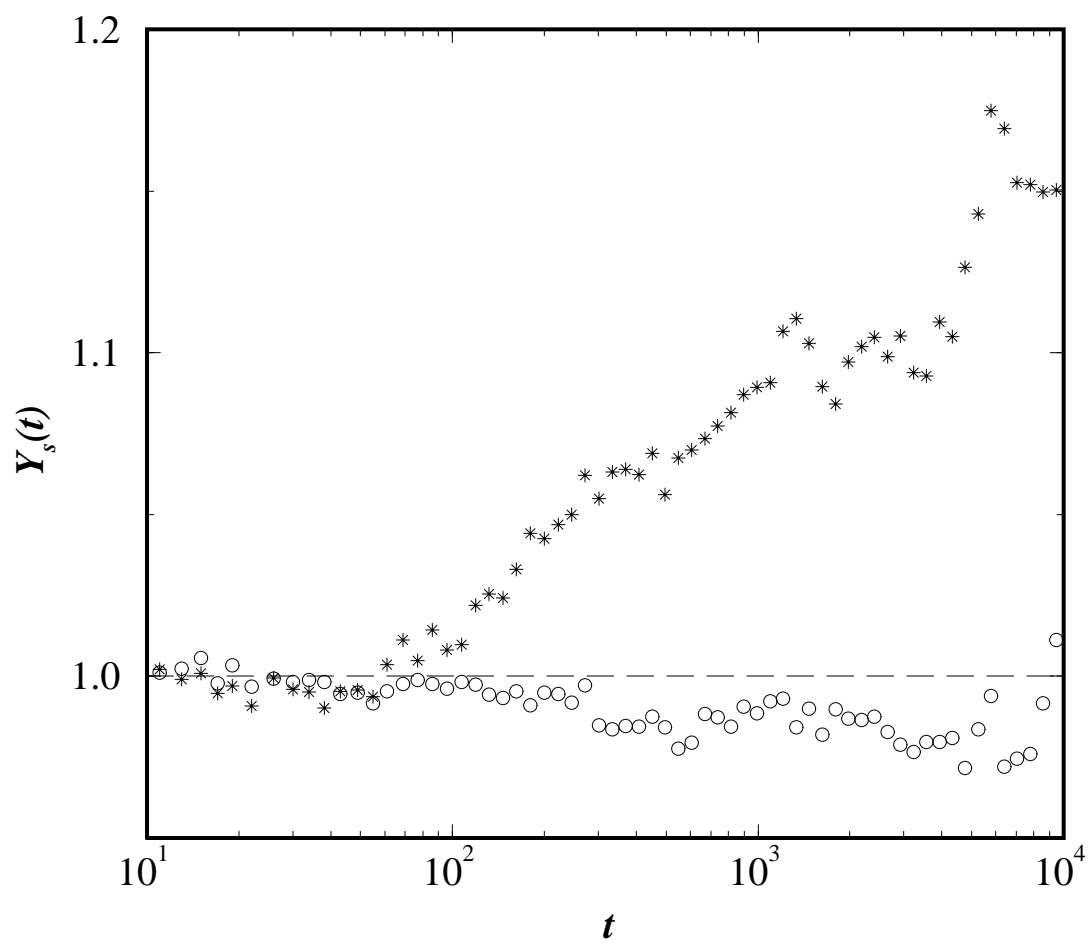
T. J. da Silva and J. G. Moreira - Figure 2



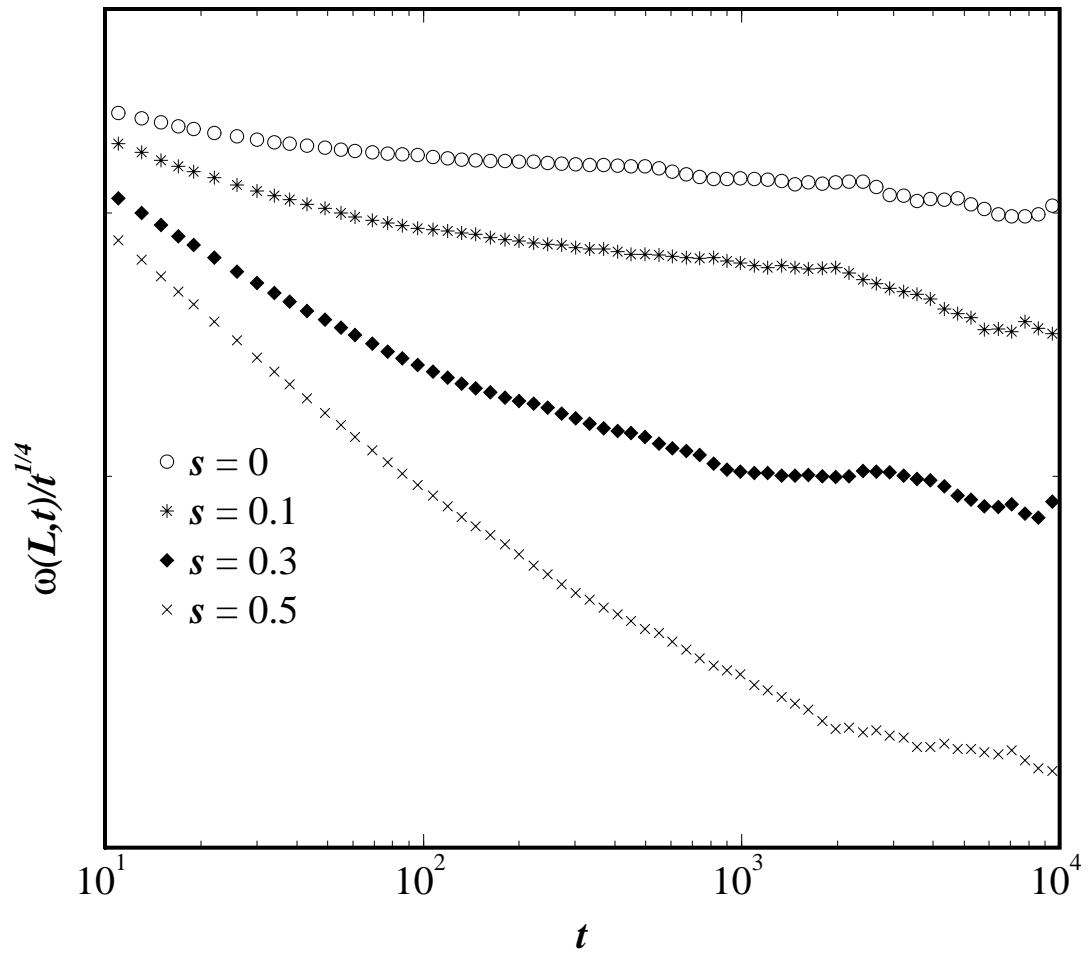
T. J. da Silva and J. G. Moreira - Figure 3



T. J. da Silva and J. G. Moreira - Figure 4



T. J. da Silva and J. G. Moreira - Figure 5



T. J. da Silva and J. G. Moreira - Figure 6